

Collision avoidance strategies for quadrotors in tight formation flying*

Shai Arogeti¹ and Amit Ailon²

Abstract—The paper proposes controllers for a multi-Quad system that flies in a tight rigid formation. The considered model of the aerial vehicle are highly nonlinear. We propose a control strategy for avoiding collision between neighboring vehicles. The collision avoidance strategy applies in particular the flatness property of the considered system. Simulation results which demonstrate the controller effectiveness, are presented.

Index Terms- Quadrotor, nonlinear model, flatness, formation control, collision avoidance.

I. INTRODUCTION

The flying robot quadrotor-helicopter (Quad in short) is an emerging rotorcraft concept in the field of small scale aerial platforms. Examples of research papers that deal with various control aspects of the Quad systems are [5], [6], [7], [15], and [18]. However, there are still many open challenging control problems in the Quad-type helicopters.

Formation control of multiple autonomous vehicles has received in the last decade an increasing interest in the control community. Works in this area are generally inspired by the recent results in the coordinated control of multi-agent systems. Related research topics include flocking of mobile autonomous agents [16], [10] and coordination and consensus problems [19].

The topic of formation flight control for small scale autonomous helicopters has been considered in [20], [9], [13], and [14]. In [2] low level controllers have been proposed for a group of Quads that fly in formation, in particular in a string-like flight pattern. Here we are concentrating on control of a rigid formation of a group of Quads Fig. 1 and establish control strategy for collision avoidance.

In this regard we assume that the needed information can be measured and communicated in real time to the controlled vehicles. We consider here the highly nonlinear model of the Quad. The current formation control strategies are based on some results in [1] regarding the trajectory tracking algorithms for Quads. The concept of flatness [11] will be applied for designing a reference trajectories to each vehicle in the group. We apply also the concepts of *virtual vehicle* and *virtual formation*. The virtual formation is constructed abstractly by a group of virtual Quads and the

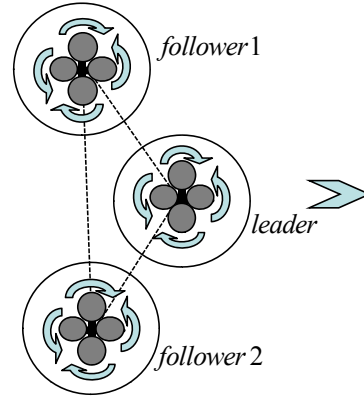


Fig. 1. Three Quads in rigid formation flight.

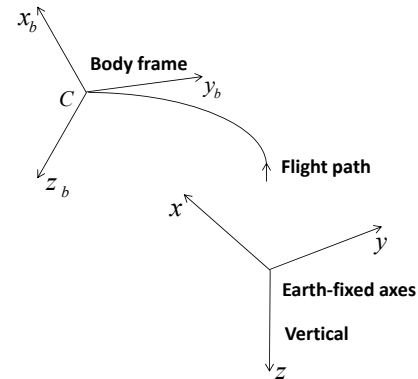


Fig. 2. The earth-fixed and body frames. The center of mass (C) is the body frame's origin.

controller objective is to force the real Quads to fly towards the corresponding virtual ones.

II. PRELIMINARIES

A. Modeling

We assume in this study knowledge of the real values of the system's parameters. The aerial vehicle and its payload are regarded as a rigid body. The rotor gyroscopic effects are neglected.

Let the inertial coordinate system in Fig. 2 be assigned by $\{x, y, z\}$ and the rigid body coordinate system by $\{x_b, y_b, z_b\}$. The origin of the rigid body frame is located at the rigid body mass center.

*This work was not supported by any organization

¹Shai Arogeti is with Dept. of Mechanical Engineering, Faculty of Engineering Science, Ben Gurion University of the Negev, Beer Sheva 84105, Israel. Email: arogeti@bgu.ac.il.

²Amit Ailon is with Dept. of Electrical & Computer Engineering, Faculty of Engineering Science, Ben Gurion University of the Negev, Beer Sheva 84105, & Dept. of Electrical Engineering, Afeka Academic College of Engineering, Tel Aviv 69107, Israel. Email: amit@ee.bgu.ac.il.

Let the Euler angles be denoted by ψ, θ, ϕ . Henceforth, whenever convenient we use the shorthand notation $C_\varrho \doteq \cos \varrho$, $S_\varrho \doteq \sin \varrho$, $T_\varrho \doteq \tan \varrho$ for trigonometric functions. By using Euler angles and applying the associated sequence of rotations the center of mass velocity in the inertial coordinate system is $v_i = \mathcal{R}v_b$ where v_b is the linear velocity in the body coordinate frame and

$$\mathcal{R} = \begin{bmatrix} C_\theta C_\psi & C_\psi S_\theta S_\phi - C_\phi S_\psi & C_\psi S_\theta C_\phi + S_\phi S_\psi \\ C_\theta S_\psi & C_\phi C_\psi + S_\theta S_\phi S_\psi & -S_\phi C_\psi + S_\theta C_\phi S_\psi \\ -S_\theta & C_\theta S_\phi & C_\theta C_\phi \end{bmatrix} \quad (1)$$

Let, the Euler vector be given by $\xi = [\phi, \theta, \psi]^T$. The relation between ω_b , the angular velocity in the body coordinate frame and the rate of change of the Euler angles is given by

$$\omega_b = \begin{bmatrix} 1 & 0 & -S_\theta \\ 0 & C_\phi & C_\theta S_\phi \\ 0 & -S_\phi & C_\theta C_\phi \end{bmatrix} \dot{\xi} \doteq \mathcal{M}(\xi) \dot{\xi}. \quad (2)$$

Since $\det \mathcal{M} = \cos \theta$ provided $\theta \in (-\pi/2, \pi/2)$ we can define $\mathcal{M}^{-1}(\xi) \doteq \mathcal{L}(\xi)$ and we have $\dot{\xi} = \mathcal{L}(\xi) \omega_b$.

Finally, the twelve order Quad nonlinear dynamical model is given by ($e_3 = [0, 0, 1]^T$)

$$\begin{aligned} \dot{\varphi}_1 &= \varphi_2 \\ \dot{\varphi}_2 &= \mathcal{R}(\xi) F/m + e_3 g \\ \dot{\xi} &= \mathcal{L}(\xi) \omega_b \\ \dot{\omega}_b &= J^{-1} \mathcal{S}(J \omega_b) \omega_b + J^{-1} M \end{aligned} \quad (3)$$

where $\varphi_1 = [x_1, y_1, z_1]^T \doteq [x, y, z]^T$ is the position vector of the point C (Fig. 2) in terms of the earth-fixed frame, $\varphi_2 \doteq [x_2, y_2, z_2]^T$, $\mathcal{S}(\cdot)$ is the skew-symmetric matrix with $\mathcal{S}(a)b = a \times b = -b \times a$, F and M are the applied force and moments in the body frame, g is the gravitational field acceleration, and m and J are the aircraft mass and moment of inertia, respectively.

Let f_i be the thrust force provided to the Quad by the i -th motor. Then $f_i = b\Omega_i^2$, $i = 1, 2, 3, 4$ where $b > 0$ is the trust factor and Ω_i is the angular speed of the motor i and M and F are given by (note that F aligns with the negative direction of z_b in Fig. 2)

$$\begin{aligned} M &= [lb(\Omega_1^2 - \Omega_3^2), lb(\Omega_4^2 - \Omega_2^2), \\ &\quad d(\Omega_1^2 + \Omega_3^2 - \Omega_2^2 - \Omega_4^2)]^T \\ F &= [0, 0, -U_b]^T; U_b \doteq b \sum_{i=1}^4 \Omega_i^2 \end{aligned} \quad (4)$$

where l is the distance from the motors to the point C and d is the drag factor [3] and [4]. Alternatively to (4) one may write

$$[U_b, M^T]^T = H [\Omega_1^2, \Omega_2^2, \Omega_3^2, \Omega_4^2]^T \quad (5)$$

where $H \in \mathbb{R}^{4 \times 4}$ is a nonsingular constant matrix.

For further consideration we need the following change of variables. Since $\omega_b = \mathcal{M}(\xi) \dot{\xi}$ we have $\dot{\omega}_b =$

$\dot{\mathcal{M}}(\xi) \dot{\xi} + \mathcal{M}(\xi) \ddot{\xi}$. Hence, (3) can be rewritten as (recall that $\mathcal{L}(\xi) \doteq \mathcal{M}^{-1}(\xi)$ and $\theta \in (-\pi/2, \pi/2)$)

$$\begin{aligned} \dot{\varphi}_1 &= \varphi_2 \\ \dot{\varphi}_2 &= \begin{bmatrix} -C_\psi S_\theta C_\phi - S_\phi S_\psi \\ S_\phi C_\psi - S_\theta C_\phi S_\psi \\ -C_\theta C_\phi \end{bmatrix} m^{-1} U_b + \begin{bmatrix} 0 \\ 0 \\ g \end{bmatrix} \\ \dot{\xi}_1 &= \xi_2 \\ \dot{\xi}_2 &= [-\mathcal{H} + \mathcal{L} J^{-1} \mathcal{S}(J \mathcal{M} \xi_2)] \mathcal{M} \xi_2 + \mathcal{L} J^{-1} M \end{aligned} \quad (6)$$

where $\xi_1 \doteq \xi = [\phi, \theta, \psi]^T$, $\varphi_1 = [x_1, y_1, z_1]^T \doteq [x, y, z]^T$, $\varphi_2 = \dot{\varphi}_1 = [x_2, y_2, z_2]^T$, and $\mathcal{H}(\xi_1, \xi_2) = \mathcal{L}(\xi_1) \dot{\mathcal{M}}(\xi_1) \mathcal{L}(\xi_1)$.

B. Trajectory tracking

Before we consider the formation control problems, it is useful to consider the trajectory tracking problem of the Quad system. To this end we recall the flatness property [11] with regard to the system (6) with the state vector $\chi = [\xi_1^T, \xi_2^T, \varphi_1^T, \varphi_2^T]^T$ and input $U = [U_b, M^T]^T$. A system is flat if one can find an output (possibly fictitious) such that all states and inputs can be determined from this output and its derivatives. Previous papers, e.g. [22], [17], [21], and [1] have been shown that the Quad system is flat. To this end let

$$y_f^*(t) = [\varphi_1^{*T}(t), \psi^*(t)]^T, t \geq 0 \quad (7)$$

be a sufficiently smooth vector-valued function with $\varphi_1^* = [x_1^*, y_1^*, z_1^*]^T = [x^*, y^*, z^*]^T$ subject to $\sup \{\ddot{z}^*(t) : t > 0\} \leq g - \varpi$ for some (arbitrarily selected) $\varpi \in (0, g)$ and $\psi^*(t) \in (-\pi/2, \pi/2)$. (Note that the upward direction of the z axis in Fig. 2 is negative and thus the last condition implies that free-fall motion is not allowed.) Then (see [1]) a trajectory $\chi^*(t) = [\varphi_1^{*T}(t), \varphi_2^{*T}(t), \xi_1^{*T}(t), \xi_2^{*T}(t)]^T$ and an input $U^*(t) = [U_b^*(t), M^{*T}(t)]^T$ subject to $U_b^*(t) > 0$ can be determined by $y_f^*(t)$ and its derivatives such that the pair $\{\chi^*(t), U^*(t)\}$ satisfies (6).

Let a sufficiently smooth time parameterized path be given (in terms of *earth frame*) by $\varphi_1^*(t) = [x_1^*(t), y_1^*(t), z_1^*(t)]^T$ with $\sup \{\ddot{z}_1^*(t) : t > 0\} \leq g - \varpi$ for an arbitrarily selected $\varpi \in (0, g)$. The control objective is to find a control law $U(t) = [U_b(t), M^T(t)]^T$ with $U_b(t) > 0$ that ensures in (6) $\varphi_i(t) \rightarrow \varphi_i^*(t)$, $i = 1, 2$ where $\varphi_2^*(t) \doteq [x_2^*(t), y_2^*(t), z_2^*(t)]^T$. The trajectory tracking controller presented in [1] is useful in the current formation control strategy. Without entering into details the tracking controller is taken from [1] as follows. Define

$$\begin{aligned} \rho_1 &= -\dot{x}_2^*/C_\psi + a_1 \tanh(\alpha(x_1 - x_1^*) + \beta(x_2 - x_2^*)) \\ &\quad + a_2 \tanh(\beta(x_2 - x_2^*)) \\ \sigma_1 &= \dot{y}_2^*/C_\psi - b_1 \tanh(\gamma(y_1 - y_1^*) + \delta(y_2 - y_2^*)) \\ &\quad - b_2 \tanh(\delta(y_2 - y_2^*)) \\ \rho_2 &= -\dot{z}_2^* + c_1 \tanh(\rho(z_1 - z_1^*) + \eta(z_2 - z_2^*)) \\ &\quad + c_2 \tanh(\eta(z_2 - z_2^*)) \end{aligned} \quad (8)$$

where $a_i, b_i, c_i, \alpha, \beta, \gamma, \delta, \rho, \eta > 0$ with $c_1 + c_2 < \varpi$ for $\varpi \in (0, g)$. Let the thrust force U_b be taken as

$$U_b = m \sqrt{\rho_1^2 + (\rho_2 + g)^2} / \cos \phi \doteq m \bar{U}_b / C_\phi \quad (9)$$

and define

$$\begin{aligned} \phi_d &\doteq \arctan \left[\sigma_1 / \sqrt{\rho_1^2 + (\rho_2 + g)^2} \right] \\ \theta_d &\doteq \arctan [\rho_1 / (\rho_2 + g)]; \psi_d \doteq 0. \end{aligned} \quad (10)$$

Note that using the flatness property the *yaw angle* ψ is forced to track $\psi_d(t) = \psi^*(t) = 0$. Since $-\dot{z}_1^*(t) - c_1 - c_2 + g > 0 \rightarrow \rho_2 + g > 0$ we have $\phi_d, \theta_d \in (-\pi/2, \pi/2)$.

Consider (10), set $\xi_d = [\phi_d, \theta_d, \psi_d]^T \doteq \xi_{1d}, \xi_{2d} \doteq \dot{\xi}_d$ and

$$T \doteq \dot{\xi}_{2d} - D_1 (\xi_1 - \xi_{1d}) - D_2 (\xi_2 - \xi_{2d}) \quad (11)$$

where $D_i \in \mathbb{R}^{3 \times 3}$ with $D_i = D_i^T > 0$. Recall that $\mathcal{L} = \mathcal{M}^{-1}$ and $\mathcal{H} = \mathcal{L} \dot{\mathcal{M}} \mathcal{L}$ let

$$M = J \mathcal{M} (T + [\mathcal{H} - \mathcal{L} J^{-1} \mathcal{S} (J \mathcal{M} \xi_2)] \mathcal{M} \xi_2). \quad (12)$$

Defining the error vectors $\mu_1 \doteq \xi_1 - \xi_{1d}$, $\mu_2 \doteq \xi_2 - \xi_{2d}$, $e_1 = [e_{11}, e_{12}, e_{13}]^T = \varphi_1 - \varphi_1^*$, and $e_2 = [e_{21}, e_{22}, e_{23}]^T = \varphi_2 - \varphi_2^*$ where $\varphi_i = [x_i, y_i, z_i]^T$, $\varphi_i^* = [x_i^*, y_i^*, z_i^*]^T$, $i = 1, 2$ and substituting the right-hand sides of (9) and (11)-(12) for U_b and M respectively in (6) we arrive at

$$\begin{aligned} \dot{e}_1 &= e_2 \\ \dot{e}_2 &= \begin{bmatrix} -[a_1 \tanh(\alpha e_{11} + \beta e_{21}) + a_2 \tanh(\beta e_{21})] C_\psi \\ -\bar{U}_b (S_\theta - S_{\theta_d}) C_\psi - \bar{U}_b T_\phi S_\psi \\ -[b_1 \tanh(\gamma e_{12} + \delta e_{22}) + b_2 \tanh(\delta e_{22})] C_\psi \\ + \bar{U}_b (T_\phi - T_{\phi_d}) C_\psi - \bar{U}_b S_\theta S_\psi \\ -[c_1 \tanh(\lambda e_{13} + \eta e_{23}) + c_2 \tanh(\eta e_{23})] \\ - \bar{U}_b (C_\theta - C_{\theta_d}) \end{bmatrix} \\ \dot{\mu}_1 &= \mu_2 \\ \dot{\mu}_2 &= -D_1 \mu_1 - D_2 \mu_2. \end{aligned} \quad (13)$$

Then, [1] shows that the trivial solution of the system (13) is asymptotically stable and $\varphi_i \rightarrow \varphi_i^*$ for $i = 1, 2$.

III. FORMATION CONTROLS

A. Constructing a virtual rigid formation

This section is devoted to the control problem of N Quads Ξ_i that follow a leader Ξ_0 and form together a *rigid formation* (in a constant altitude h) The objective is to control a group of Quads so that they behave as if they were particles embedded in a rigid structure. The formation leading Quad flies along a predetermined time-parameterized smooth path. For achieving the control goal we employ the concept of virtual formation. The virtual formation is constructed by N virtual Quads that "follow" the real leader Ξ_0 . The trajectory tracking controller will force the real aerial vehicle to follow the reference trajectory which is represented by the corresponding virtual Quad.

At this point we need introduce a moving frame denoted by $\{x_m, y_m, z_m\}_m$ that will allow us to determine the virtual formation. The moving frame $\{\}_m$ satisfies the following conditions. 1.- The origins of the frame $\{x_m, y_m, z_m\}_m$

and the body frame $\{x_b, y_b, z_b\}_b$ (the point C in Fig. 2) coincide, 2.- the subspace $\{x_m, y_m\}_m$ is always parallel to the subspace $\{x, y\}_i$ in the earth frame, and 3.- the axis x_m is always tangential to a desired time-parametrized path \mathbb{C} at the moving point C .

Let $\mathbb{C}: \varphi_1^*(t) = [x_1^*(t), y_1^*(t), h]^T$ be the leader smooth time-parameterized path. Suppose that the *virtual formation* has been set up, namely, each virtual vehicle Ξ_i^* (a point in $\{\}_m$) 'flies' in a designated location with respect to the leader Ξ_0 . In order to establish the error dynamics for each pair of real-virtual Quads $\{\Xi_i, \Xi_i^*\}$, we need to characterize the motion of Ξ_i^* in terms of the inertial frame, given the time parameterized path of the leader. To this end let $\eta(t)$ be the rotation angle between the (parallel) frames $\{x_m, y_m\}_m$ and $\{x, y\}_i$ at t (i.e. direction of the tangent vector to the curve \mathbb{C} at t). Then, rotation matrix between the frames $\{x_m, y_m\}_m$ and $\{x, y\}_i$ is

$$\mathcal{R}_\eta(t) = \begin{bmatrix} \cos \eta(t) & -\sin \eta(t) \\ \sin \eta(t) & \cos \eta(t) \end{bmatrix}. \quad (14)$$

Let $o_i^* = [\xi_i, \gamma_i]^T$ be a vector from the moving origin C to Ξ_i^* in the system $\{\}_m$. Recalling that $\varphi_1^*(t) = [x_1^*(t), y_1^*(t), h]^T$ is the vector-valued function for C in terms of the inertial frame and using a *rigid motion transformation* the vector r_i^* of o_i^* in terms of $\{x, y, z\}_i$ is given by

$$r_i^*(t) = \begin{bmatrix} \mathcal{R}_\eta(t) [\xi_i, \gamma_i]^T \\ h \end{bmatrix} + \varphi_1^*(t) \doteq \begin{bmatrix} r_{xi}^*(t) \\ r_{yi}^*(t) \\ h \end{bmatrix}. \quad (15)$$

B. Controller for a rigid formation

Considering the virtual formation that follows the leader Ξ_0 , the group of the real Quads will succeed in accomplishing its task by applying the trajectory tracking control algorithm such that $\Xi_i \rightarrow \Xi_i^*$ for each pair $\{\Xi_i, \Xi_i^*\}$. To this end we recall that for each vehicle Ξ_i the tracking controller is based on (8) and (10) with $\xi_{1di} \doteq \xi_{di} = [\phi_{di}, \theta_{di}, \psi_{di}]^T$, $\xi_{2di} \doteq \dot{\xi}_{di}$ and $\dot{\xi}_{2di} \doteq \ddot{\xi}_{di}$, which determine T_i in (11) and hence M_i in (12) for $i = 1, 2, \dots, N$.

Consider (8) and (10) and let (recall that we consider flight in a constant altitude, $z_{1i} = z_{1i}^* = h \rightarrow \dot{z}_{1i} = \dot{z}_{1i}^* = 0$)

$$\begin{aligned} \rho_{1i} &= -\ddot{x}_{1i}^*/C_\psi + a_1 \tanh(\alpha(x_1 - x_i^*) + \beta(x_2 - x_{2i}^*)) \\ &\quad + a_2 \tanh(\beta(x_2 - x_{2i}^*)) \\ \sigma_{1i} &= \ddot{y}_{1i}^*/C_\psi - b_1 \tanh(\gamma(y_1 - y_{1i}^*) + \delta(y_2 - y_{2i}^*)) \\ &\quad - b_2 \tanh(\delta(y_2 - y_{2i}^*)) \\ \rho_{2i} &= 0 \end{aligned} \quad (16)$$

for $i = 1, 2, \dots, N$. Using (16) and (9)-(10) we set

$$U_{bi} = m \sqrt{\rho_{1i}^2 + g^2} / \cos \phi_i \doteq m \bar{U}_{bi} / C_{\phi_i} \quad (17)$$

and define

$$\begin{aligned} \phi_{di} &\doteq \arctan \left[\sigma_{1i} / \sqrt{\rho_{1i}^2 + g^2} \right] \\ \theta_{di} &\doteq \arctan [\rho_{1i} / g] \\ \psi_{di} &\doteq 0. \end{aligned} \quad (18)$$

Recalling that $\xi_{di} = [\phi_{di}, \theta_{di}, \psi_{di}]^T$ and $\xi_{1di} \doteq \xi_{di}$, $\xi_{2di} \doteq \xi_{di}$, and $\xi_{2di} \doteq \xi_{di}$, the applied torques M_i (see (11)-(12))

$$T_i \doteq \dot{\xi}_{2di} - D_1 (\xi_{1i} - \xi_{1di}) - D_2 (\xi_{2i} - \xi_{2di}) \quad (19)$$

where $D_i \in \mathbb{R}^{3 \times 3}$ with $D_i = D_i^T > 0$. Using $\mathcal{L} = \mathcal{M}^{-1}$ and $\mathcal{H} = \mathcal{L}\mathcal{M}\mathcal{L}$ let

$$M_i = J\mathcal{M} (T_i + [\mathcal{H} - \mathcal{L}J^{-1}\mathcal{S} (J\mathcal{M}\xi_{2i})] \mathcal{M}\xi_{2i}). \quad (20)$$

Defining the error vectors $\mu_{1i} \doteq \xi_{1i} - \xi_{1di}$, $\mu_{2i} \doteq \xi_{2i} - \xi_{2di}$, $e_{1i} = [e_{11i}, e_{12i}, e_{13i}]^T = \varphi_{1i} - \varphi_{1i}^*$, and $e_{2i} = [e_{21i}, e_{22i}, e_{23i}]^T = \varphi_{2i} - \varphi_{2i}^*$ where $\varphi_{1i} = [x_i, y_i, z_i]^T$, $\varphi_{1i}^* = [x_i^*, y_i^*, z_i^*]^T$, $i = 1, 2$ and substituting the right-hand sides of (17) and (19)-(20) for U_{bi} and M_i respectively in (6), (13) becomes

$$\begin{aligned} \dot{e}_{1i} &= e_{2i} \\ \dot{e}_{2i} &= \begin{bmatrix} -[a_1 \tanh(\alpha e_{11i} + \beta e_{21i}) + a_2 \tanh(\beta e_{21i})] C_{\psi i} \\ -\bar{U}_{bi}(S_{\theta i} - S_{\theta di}) C_{\psi i} - \bar{U}_{bi} T_{\phi i} S_{\psi i} \\ -[b_1 \tanh(\gamma e_{12i} + \delta e_{22i}) + b_2 \tanh(\delta e_{22i})] C_{\psi i} \\ +\bar{U}_b(T_{\phi i} - T_{\phi di}) C_{\psi i} - \bar{U}_{bi} S_{\theta i} S_{\psi i} \\ -[c_1 \tanh(\lambda e_{13i} + \eta e_{23i}) + c_2 \tanh(\eta e_{23i})] \\ -\bar{U}_{bi}(C_{\theta i} - C_{\theta di}) \end{bmatrix} \\ \dot{\mu}_{1i} &= \mu_{2i} \\ \dot{\mu}_{2i} &= -D_{1i}\mu_{1i} - D_{2i}\mu_{2i}. \end{aligned}$$

IV. COLLISION AVOIDANCE IN CLOSE FORMATION FLYING

Since in real situations the Quads are subject to sensor, actuator, and communication constraints and failures, a sensor-based algorithms for collision avoidance and control switching should support the controllers in real time [8] and [12]. Here we consider the following obstacle avoidance control strategy, which is based on the flatness property of the considered system.

Roughly, each follower 'sees' a potential obstacle (a neighboring Quad) with an enclosed circle that designates a forbidden area and moves together with the obstacle. Once the follower is approaching the forbidden region a motion planning algorithm is taking place such that the Quad position never crosses into the forbidden region and thus guaranteeing safe bypassing of a moving obstacle and yet to ensure a safe return to the desired location for maintaining the formation geometry.

We illustrate the considered approach by Fig. 3 which demonstrates 6 Quads flying in a formation in a horizontal plane. The rounded boarder enclosing a Quad designates a forbidden region for neighboring vehicles. Consider now a scenario where Quad *follower 1* is too close to the forbidden region associated with the leader and its velocity vector (the red arrow in Fig. 3) points towards the leader. Then, the system needs to recruit an emergency control strategy for avoiding collision (for the sake of illustration see the green arrow in Fig. 3). Once this happens the control law of the Quad *follower 1* switches to an evasion strategy. Of course, the original formation pattern is then temporarily changing and thus the controller should provide

simultaneously a control mode that carefully regenerating the converging motion towards the desired relative position in the formation.

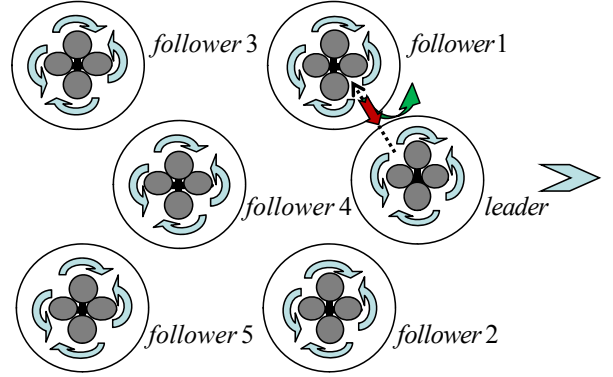


Fig. 3. A six-Quad flying formation in a horizontal plane: a collision avoidance scenario.

Formally we apply the following strategy for collision avoidance. Let the position vectors of vehicles Ξ_i and Ξ_{i-1} (the higher index designates the maneuvering Quad) be respectively $r_i = [x_i, y_i, z_i]^T$ and $r_{i-1} = [x_{i-1}, y_{i-1}, z_{i-1}]^T$. We consider the input signals that applies to vehicle Ξ_i for avoiding collision. Consider the vector $d = [x_{i-1} - x_i, y_{i-1} - y_i, z_{i-1} - z_i]^T$. The collision avoidance control procedure is enabled once $\|d\| < d^*$ where $d^* > 0$ is some predetermined constant. For the sake of notation simplicity we omit in the following the sub-index i associated with vehicle Ξ_i . Define:

$$a_d = \begin{bmatrix} -C_{\psi d} S_{\theta d} C_{\phi d} - S_{\phi d} S_{\psi d} \\ S_{\phi d} C_{\psi d} - S_{\theta d} C_{\phi d} S_{\psi d} \\ -C_{\theta d} C_{\phi d} \end{bmatrix} m^{-1} U_b + \begin{bmatrix} 0 \\ 0 \\ g \end{bmatrix} \quad (21)$$

where (see (17)-(18) and recall that we consider flight in the horizontal plan which means that $\rho_2 = 0$ in (8))

$$\begin{aligned} \phi_d &\doteq \arctan \left[\sigma_1 / \sqrt{\rho_1^2 + g^2} \right] \\ \theta_d &\doteq \arctan [\rho_1 / g] \\ \psi_d &\doteq 0 \\ U_b &= m \sqrt{\rho_1^2 + g^2} / C_\phi \doteq m \bar{U}_b / C_\phi \end{aligned} \quad (22)$$

The vector a_d in (21) represents the acceleration towards the desired trajectory. Once $\|d\| < d^*$ the controller needs to reduce effectively the magnitude of the projection of a_d along the direction of the unit vector $\hat{d} = d / \|d\|$. This will be accomplished by increasing the component of a_d in the negative direction of \hat{d} , namely,

$$\begin{aligned} e_d &= d^* - \|d\| \\ a_d^{\parallel} &= (-k_1 e_d - k_2 \dot{e}_d) \hat{d} \end{aligned} \quad (23)$$

where the positive constants k_i are weighting factors that dominate the magnitude of the acceleration in the $-\hat{d}$ direction. However, as far as the projection of a_d along the

orthogonal direction to \hat{d} is concerned, namely,

$$a_d^\perp = \left(I_3 - \hat{d}\hat{d}^T \right) a_d \quad (24)$$

this vector ensures that the aircraft proceed its flight with the group. Finally, the acceleration

$$\begin{bmatrix} \ddot{x}^* \\ \ddot{y}^* \\ 0 \end{bmatrix} = a_d^\perp + a_d^\parallel \quad (25)$$

establishes the evasion dynamics under the enforcement emergency scenarios.

We are now in a position to apply the flatness property (Subsection 2.2) for realizing the proposed collision avoidance procedure. By flatness we can realize the evasive trajectory by implementing the inputs $F_b^*(t) = [0, 0, -U_b^*(t)]^T$ and $M_b^*(t)$ which are determined by (25). In particular using the formulation in [1] we have

$$\begin{aligned} U_b^*(t) &= \sqrt{\ddot{x}^{*2}(t) + \ddot{y}^{*2}(t) + (\ddot{z}^*(t) - g)^2} \\ \phi^*(t) &= \arcsin [f_x^*(t) \sin \psi^*(t) - f_y^*(t) \cos \psi^*(t)] \\ f_x^*(t) &= -\ddot{x}^*(t)/U_b^*(t), \quad f_y^* = -\ddot{y}^*(t)/U_b^*(t) \\ \theta^*(t) &= \arcsin [(f_x^*(t) \cos \psi^*(t) \\ &\quad + f_y^*(t) \sin \psi^*(t)) / \cos \psi^*(t)] \end{aligned} \quad (26)$$

and once $\xi^*(t) = [\phi^*(t), \theta^*(t), \psi^*(t)]^T$ is well-defined, the nominal torque $M^*(t)$ can be computed by the last two equations of (3), or equivalently by the last two equations of (6) with the starred variables. Hence a nominal evasion trajectory and inputs are realizing.

Remark. The above procedure for collision avoidance can be applied simultaneously to two or more aerial vehicles, which are about to collide while flying in a tight rigid formation.

V. EXAMPLES

Based on the analytical approach we demonstrate the controller performance for the flying three-Quad arrowhead rigid formation in Fig. 1 while applying the algorithm for collision avoidance.

The Quads physical parameters are the same (we use the MKS units system): the mass $m = 1$, the inertia moment (for simplicity assume a diagonal matrix) $J = \text{diag}[0.125/4, 0.125/4, 0.250/4]$. The controller parameters (see (8) and (11)) are $a_1 = a_2 = b_1 = b_2 = c_1 = c_2 = 1$, $\alpha = \beta = \gamma = \eta = \delta = 1$, $\rho = 2$, and $D_1 = D_2 = \text{diag}[5, 5, 5]$. The desired offset of follower 1 in Fig. 1 is (see Subsection 3.1) $o_1^* = [\xi_1, \gamma_1]^T = [-1, 1]^T$ and its position initial conditions are: $x(0) = 10$, $y(0) = 0$, $z(0) = 4$ and the other state variable initial conditions are all zeros. The desired offset of follower 2 is $o_2^* = [\xi_2, \gamma_2]^T = [-1, -1]^T$. The parameters for the collision avoidance control scheme (see the discussion above and equation (23)) $d^* = 1.5$, and $k_1 = 2.5$, $k_2 = 0.8$.

The leader path is given in a parametric form: $x(t) = 10 \cos(0.2t)$, $y(t) = 10 \sin(0.2t)$, $z(t) = -5$ (note the upward direction of the negative direction of the z coordinate

in Fig. 2). The initial conditions of the leader are $x(0) = y(0) = 0$, $z(0) = -5$. The initial conditions of *follower 1* are $x(0) = 12$, $y(0) = 2$, $z(0) = -5$ and the initial conditions of *follower 2* are $x(0) = 8$, $y(0) = -1$, $z(0) = -5$. All other state variable initial conditions are all zeros.

Two flight scenarios are demonstrated through a set of figures as follows. The Quad trajectories during convergence to the desired formation is presented in Fig. 4. In the first example the collision avoidance controller is inactive, and the two followers collide while converging from their initial positions to the desired ones in the flying formation. This situation is clearly understood from Fig. 5 that shows the distance between the two followers; after 4.7sec. from the beginning, the distance between the two followers is zero. In the second example we apply the collision avoidance strategy. The collision avoidance controller is activated whenever the distance between two Quads is smaller than 1.5m. As can be seen from Fig. 6, the actual trajectory exhibits now an evasion maneuver mode of follower 2 for avoiding collision with follower 1. In Fig. 6, the thick portions of the blue curve show where the collision avoidance controller is active in follower 2. In this simulation, the collision avoidance algorithm is required to be used twice, and in both cases the distance between the two followers is kept above 1m (as shown in Fig. 7). The control signals of follower 2 in the second simulation are presented in Fig. 8. The two time sections colored with grey show the control signals when the collision avoidance algorithm is active.

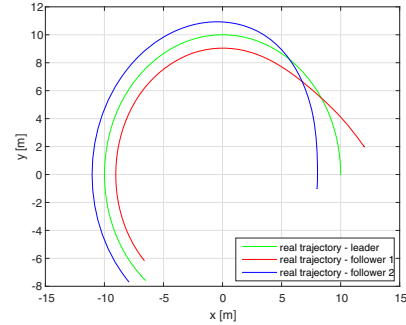


Fig. 4. Example 1: Top view of the Quads while converging to the arrowhead rigid formation. The collision avoidance controller is inactive and *followers 1 and 2* collide.

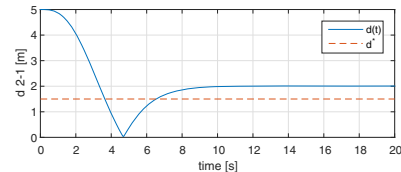


Fig. 5. Example 1: d_{21} is the distance between the *followers 1 and 2* and $d^* = 1.5$. At $t = 4.7$ sec. the two vehicles collide.

VI. CONCLUSION

The paper presents formation control strategies for Quad helicopters with the highly nonlinear model. The proposed

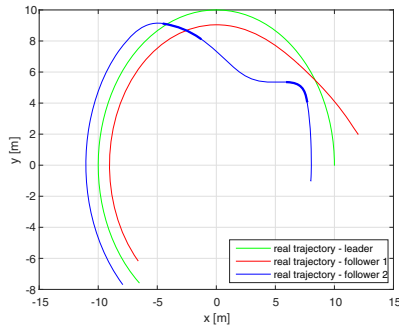


Fig. 6. Example 2: Top view of the Quads while converging to the arrowhead rigid formation. The collision avoidance controller is active and follower 2 evades collision (see the thick portions of the blue curve).

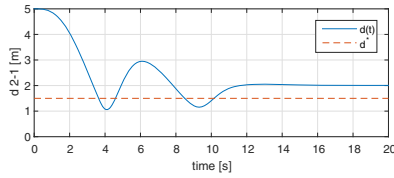


Fig. 7. Example 2: The collision avoidance algorithm is active whenever $d_{21} \leq d^* = 1.5$.

control algorithms are based on the flatness property and the concepts of virtual vehicles and virtual formations. The proposed control strategy allows formation maneuvers, splitting, and merging. The control law satisfies also a predefined timing-law that determines the formation rate of advancement. The issue of collision avoidance has been considered and control laws which allow to formulate the maneuver for collision avoidance have been established. Simulation results demonstrate the effectiveness of the proposed controllers.

REFERENCES

[1] A. Ailon, "Closed-form feedback controllers for set-point and trajectory tracking for the nonlinear model of quadrotor helicopters," *Proceedings of the 7th IFAC Symposium on Robust Control Design (ROCOND)*, Aalborg, Denmark, June 2012.

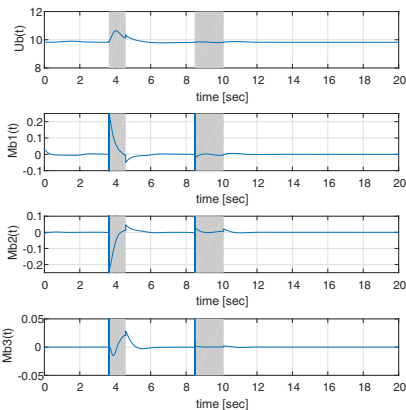


Fig. 8. Example 2: The collision avoidance control algorithm of follower 2 is active during the two time periods designated with grey backgrounds.

[2] A. Ailon and S. Arogeti, "Formation control strategies for autonomous quadrotor-type helicopters," *Proceedings of the 2nd IFAC Workshop on Research, Education and Development of Unmanned Aerial Systems*, Compiegne, France, November 2013.

[3] S. Bouabdallah, P. Murrieri, and R. Siegwart, "Design and control of an indoor micro quadrotor," *Proceedings of the Int. Conf. on Rob. & Autom.*, Barcelona, Spain, April 2005.

[4] S. Bouabdallah, S. and R. Siegwart, "Full control of a quadrotor," *Proceedings of the IEEE/RSJ Int. Conf. Intel. Rob. Syst.*, San Diego, USA, October 2007.

[5] P. Castillo, A. Dzul, and R. Lozano, "Real-time stabilization and tracking of a four-rotor mini rotorcraft," *IEEE Trans. Contr. Syst. Tech.*, vol. 12, pp. 510-517, 2004.

[6] P. Castillo, R. Lozano, A. Dzul, "Stabilization of a mini rotorcraft with four rotors," *IEEE Contr. Syst. Magazine*, vol. 25, pp. 45-55, 2005.

[7] A. Das, F. Lewis, K. Subbarao, "Backstepping approach for controlling a quadrotor using Lagrange form dynamics," *J. Intel. Rob. Syst.*, vol. 56, pp. 127-151, 2009.

[8] A. K. Das, R. Fierro, V. Kumar, J. P. Ostrowski, J. Spletzer, and C. J. Taylor, "A vision-based formation Control Framework," *IEEE Trans. Rob. Autom.*, vol. 18, pp. 813-825, 2002.

[9] L. A. G. Delgado, and A. E. D. Lopez, "Formation control for quad-rotor aircrafts based on potential functions," *Proceedings of the Congreso Anual 2009 de la Asociacion de Mexico de Control Automatico (AMCA)*, Zacatecas, Mexico, September 2009.

[10] J. A. Fax, and R. M. Murray, "Information flow and cooperative control of vehicle formation," *IEEE Trans. Automat. Contr.*, vol. 49, pp. 1465-1476, 2004.

[11] M. Fliess, J. L. Levine, P. Martin, and Rouchon, "Flatness and defect of non-linear systems: introductory theory and examples," *Int. J. Control*, vol. 61, pp. 1327-1361, 1995.

[12] Masood Ghasemi, Sergey G. Nersisov, Garrett Clayton, and Hashem Ashrafioun, "Coordination control with collision avoidance for multi-agent systems with underactuated agent dynamics," *Proceedings of the Int. Conf. of Control, Dynamic Systems, and Robotics*, Ottawa, Ontario, Canada, May 2014.

[13] J. A. Guerrero, I. Fantoni, S. Salazar, and R. Lozano, "Flight Formation of Multiple Mini Rotorcraft via Coordination Control," *Proceedings of the IEEE International Conference on Robotics and Automation*, Anchorage, Alaska, USA, May 2010.

[14] J. A. Guerrero, P. Castillo, S. Salazar, and R. Lozano, "Mini rotorcraft flight formation control using bounded inputs," *J. Intell. Robot Syst.*, vol. 65, pp. 175-186, 2011.

[15] H. Huang, G. M. Hoffmann, S. L. Waslander, and C. J. Tomlin, "Aerodynamics and control of autonomous quadrotor helicopters in aggressive maneuvering," *Proceedings of the IEEE Inter. Conf. Robot. & Autom.*, Kobe, Japan, May 2009.

[16] A. Jadbabaie, J. Lin, and A. S. Morse, "Coordination of groups of mobile autonomous agents using nearest neighbour rules," *IEEE Trans. Automat. Contr.*, vol. 48, pp. 988-1001, 2003.

[17] D. Mellinger and V. Kumar, "Minimum snap trajectory and control for quadrotors" *IEEE International Conf. on Robotics and Automation (ICRA)*, Shanghai, China, May 2011.

[18] N. Michael, and V. Kumar, "Planning and control of ensembles of robots with non-holonomic constraints," *Int. J. Rob. Research*, vol. 28, pp. 962-975, 2009.

[19] R. Olfati-Saber, J. A. Fax, and R. M. Murray, "Consensus and cooperation in network multi-agent system," *Proceedings of the IEEE*, vol. 95, pp. 215-233, 2007.

[20] U. Pilz, A. Popov, and H. Werner, "Robust Controller Design for Formation Flight of Quad-Rotor Helicopters," *Proceedings of the 48th IEEE Conf. on Decision and Control*, Shanghai, China, December 2009.

[21] S. Formentin and M. Lovera, "Flatness-based control of a quadrotor helicopter via feedforward linearization," *IEEE Conf. on Decision and Control and European Control Conf.*, Orlando, USA, December 2011.

[22] N. Zhang, G. Andrei, A. Drouin, and F. Mora-Camino, "Differential flat control for rotorcraft trajectory tracking," *Proceedings of the International Multi-Conf. of Engineers and Computer Scientists*, Hong Kong, March 2009.